Evaluation of the Crystallization Kinetics and Melting of Polypropylene and Metallocene-Prepared Polyethylene Blends

Mohammad Razavi-Nouri,[1] James N. Hay[2]

[1]*Department of Plastics, Faculty of Processing, Iran Polymer and Petrochemical Institute, P.O. Box 14965/115, Tehran, Iran*
[2]*School of Engineering, Metallurgy and Materials, University of Birmingham, Edgbaston, Birmingham B15 2TT, United Kingdom*

Received 2 July 2006; accepted 14 October 2006
DOI 10.1002/app.25638
Published online in Wiley InterScience (www.interscience.wiley.com).

ABSTRACT: The kinetics of the isothermal crystallization of a polypropylene (PP) random copolymer containing 5 mol % ethylene, a metallocene linear low-density polyethylene (*m*-LLDPE) with 3.3 mol % hexene-1 as a comonomer, and three blends were studied with differential scanning calorimetry at temperatures sufficiently high to prevent any crystallization of m-LLDPE. The analysis was carried out with the Avrami equation. The overall crystallization rate and the equilibrium melting temperature of the PP copolymer decreased with increasing amounts of m-LLDPE in the blends. The former was attributed to the effect of m-LLDPE in reducing the number of primary nuclei, and the latter was attributed to a lowering of the fold surface energy due to the limited partial miscibility of the blend components. © 2007 Wiley Periodicals, Inc. J Appl Polym Sci 104: 634–640, 2007

Key words: blends; crystallization; miscibility; polyethylene (PE); poly(propylene) (PP)

INTRODUCTION

The discovery of a new family of olefin polymerization catalysts, metallocene catalysts, has opened up a new area for producing polyolefins with tailor-made chain architectures. Unlike Ziegler–Natta catalysts, which produce molecules with different chain lengths and tacticities, this group of catalysts produces copolyolefins with narrower molecular weights and controlled monomer sequence group distributions as well as variable densities.[1–3]

The blending of polypropylene (PP) and polyethylene (PE) has been an interesting research area for several decades. One reason for blending is to enhance the impact properties of PP, especially at low temperatures. On the other hand, a large volume of municipal waste consists of these two polymers, which cannot be separated from each other by a flotation method. Therefore, the investigation of the mechanical properties of PE/PP blends is necessary to determine if impurities are crucial in the recycling of polyolefins.

Although there are many published studies that have examined the miscibility and compatibility of conventional PE in PP,[4–27] few have investigated PE copolymers prepared from metallocene catalysts.[28,29] In previous works, the mechanical properties and crystallization behavior of three blends prepared from a metallocene linear low-density polyethylene (m-LLDPE) and a PP random copolymer were reported. A PP copolymer with a few molar percent of ethylene was selected to examine if the copolymerization had any effect on the compatibility of the two polymers. The results obtained from the tensile properties showed a minimum in elongation as well as an energy to break with 50% m-LLDPE in the blends. The elastic moduli of the blends were less than the values predicted by the additive rule and showed that there was an antisynergism between the two phases.[30]

Morphological and spherulite growth rate studies, carried out at different temperatures, revealed that the growth rate of the PP spherulites remained relatively unchanged and was independent of the amount of m-LLDPE studied. Optical microscopy studies also indicated that the nucleation density of the PP spherulites decreased with the introduction of m-LLDPE into PP and that m-LLDPE remained as discrete droplets dispersed throughout the intraspherulitic region of PP. In the case of a 50/50 blend, the droplets were much larger, and they formed concavities on the edges of the PP spherulites.[31]

Nonisothermal crystallization studies from the melt on cooling showed that for the m-LLDPE/PP

Correspondence to: M. Razavi-Nouri (m.razavi@ippi.ac.ir).

TABLE I
Specifications of the Materials

Name	M_w (kg/mol)[a]	M_n (kg/mol)[b]	Polydispersity index	Melt flow index (g/min)	Density (g/cm^3)	Comonomer	Comonomer content (mol %)
M-LLDPE	102.0	40.7	2.5	0.15	0.923	Hexene-1	3.3
PP (random copolymer)	365.0	101.0	3.6	0.18	0.902	Ethylene	5.0

[a] Weight-average molecular weight.
[b] Number-average molecular weight.

blends, the onset and maximum crystallization temperatures (T_C's) decreased with increasing m-LLDPE content. Two well-separated melting peaks characteristic of m-LLDPE and PP were observed, and there was no reduction in these melting points (T_m's) with the blend composition.[30]

The main goal of this work was to investigate the influence of the m-LLDPE content on the crystallization and thermal behavior of a PP copolymer in more detail. Further results are reported for some kinetic aspects with the Turnbull–Fischer theory and also for the equilibrium melting point (T_m^0) and primary nucleation process, which in the two other studies were not deeply investigated.

EXPERIMENTAL

Materials and blend preparation

The raw materials were obtained from commercial sources. PP and m-LLDPE were supplied by Himont (Ferrara, Italy) and Exxon Chemical Co. (Rueil Malmaison, France) under the trade names Moplen EP (TP-176 AM) and Exact 3009, respectively. Table I shows some of the specifications of these materials. Three blends of m-LLDPE and PP with compositions of 10/90, 30/70, and 50/50 by weight were prepared with an APV 2000 twin-screw extruder (Stoke, England) at 503 ± 5 K and a 200 rpm screw speed.

Thermal analysis

Crystallization studies were carried out with a PerkinElmer model DSC-2 differential scanning calorimeter (Beaconsfield, England) interfaced to a personal computer. The temperature scale for differential scanning calorimetry (DSC) was calibrated from the T_m values of indium, tin, and stearic acid. Each sample was heated to 473 K, held at this temperature for 5 min, and cooled at 160 K/min to T_C. Once the crystallization was completed and the DSC trace had returned to the baseline, the sample was melted to determine T_m. This was carried out at different heating rates of 5, 10, and 20 K/min, and T_m was determined by extrapolation to a zero heating rate to eliminate the effect of thermal lag. T_m^0 was determined by the Hoffman–Weeks procedure.

Optical microscopy

Measurements of the radial growth rates of PP spherulites as a function of temperature were carried out with a Leitz Dialux-Pol 50 polarized light microscope (Ernst Leitz) (Wetzlar, Germany) and a Linkam TH600 hot stage (Tadworth, England) with a PR600 temperature controller. Specimens were prepared by the placement of thin films (ca. 20 μm thick) between two glass coverslips and then inserted into the furnace of the hot stage.

A television camera and a video recorder were used to record the growth of the spherulites. The calibration of the temperature of the hot stage was achieved with T_m of zone-refined benzoic and stearic acids.

RESULTS AND DISCUSSION

Isothermal crystallization rate studies

Isothermal crystallization from the melt was studied with the Avrami equation:[32–35]

$$-\ln\left(1-\frac{X_t}{X_p}\right)=Zt^n \tag{1}$$

where Z is the primary composite rate constant incorporating the nucleation and growth rate and density, X_t is the degree of crystallinity formed only during the primary process at time t, X_p is the degree of crystallinity formed at the end of the primary process, and n is an Avrami exponent that adopts different values for different crystallization mechanisms.[36]

Taking the logarithm from eq. (1) gives

$$\log\left[-\ln\left(1-\frac{X_t}{X_p}\right)\right]=\log\ Z+n\log\ t \tag{2}$$

An average Z value was calculated from n and the half-life ($t_{1/2}$) of the primary crystallization:[32,37,38]

$$Z=\frac{\ln 2}{(t_{1/2})^n} \tag{3}$$

X_t was obtained from the ratio of the area of the exotherm up to time t divided by the total area of the exotherm:[39–43]

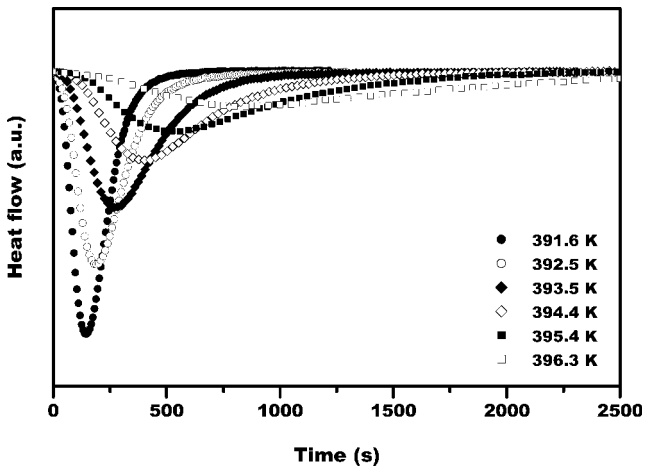

Figure 1 DSC exotherms of the isothermal crystallization of a 30/70 blend.

$$X_t = \frac{\int_0^t \frac{dH}{dt} dt}{\int_0^\infty \frac{dH}{dt} dt} \quad (4)$$

where dH/dt is the heat evolution rate.

The isothermal crystallization behavior of PP and the three blends was studied in a temperature range in which only PP was capable of crystallization and m-LLDPE remained in the molten state. For comparison, a similar study was carried out on m-LLDPE at lower T_C values. Figures 1 and 2 show the isothermal crystallization exotherms and the development of the weight fraction crystallinity of PP in a 30/70 blend, respectively. These figures show the change in the rate of crystallization and the development of the crystallinity with time and temperature and are consistent with the expected trend observed with the Avrami equation and also with nucleation control of crystallization in which the rate of crystallization decreases with increasing T_C.

The Avrami parameters were calculated for the primary crystallization of PP and the blends with eq. (2). The analysis of the primary crystallization for a 30/70 blend is shown in Figure 3. The n values for m-LLDPE and PP were found to be 2.9 ± 0.2 and 3.2 ± 0.2, respectively, and those of the blends were obtained between the two values. These are consistent with the crystallization mechanism of three-dimensional spherical growth with heterogeneous nucleation.

Figure 4 shows the $t_{1/2}$ values of the isothermal crystallization versus the temperature for PP, the blends, and m-LLDPE: they crystallized in progressively lower temperature ranges. Much longer times were required for m-LLDPE, at each temperature, to crystallize, so its crystallization could be separated from that of the PP phase by the suitable choice of T_C. A similar dependence of $t_{1/2}$ on the temperature was observed for the PP-rich blends with respect to that of PP, although it progressively shifted to lower temperatures as the m-LLDPE content increased in the blend; this was consistent with PP alone crystallizing in these samples. m-LLDPE exhibited a much higher dependence on the temperature in line with the difference in T_m^0 and the fold surface energy.

T_m^0 was calculated with the Hoffman–Weeks method[44,45] such that a plot of T_m against T_C showed a linear relationship:

$$T_m = T_m^0\left(1 - \frac{1}{2\beta}\right) + \left(\frac{1}{2\beta}\right)T_C \quad (5)$$

The intersection of the straight line with the equilibrium line $T_m = T_C$ is T_m^0, and β is the slope. β is the thickening factor, which should be 1.0 if no annealing occurs on heating to T_m and greater if annealing occurs.

Figure 5 shows plots of T_m and T_C for PP and m-LLDPE/PP blends. T_m^0 decreases with the m-LLDPE content in the blends. A depression in T_m^0 with increasing m-LLDPE is an indication of limited miscibility of

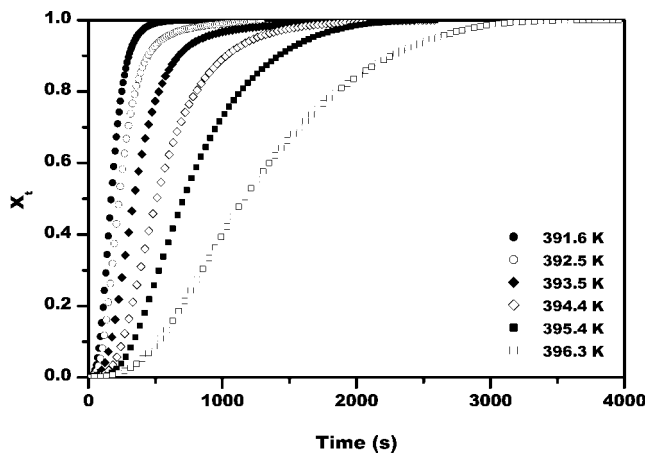

Figure 2 Development of the crystallinity with time during melt crystallization.

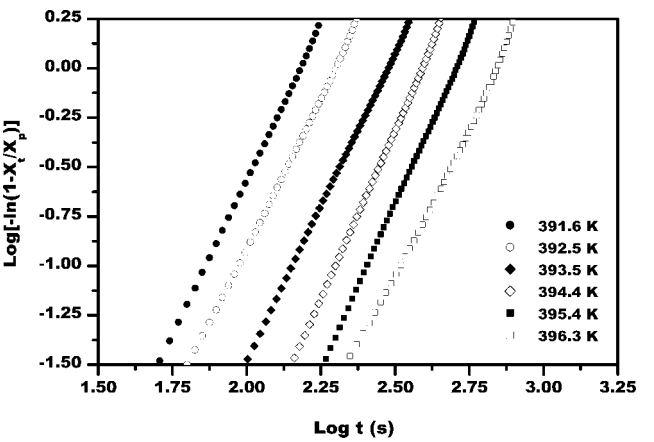

Figure 3 Avrami analysis of the primary crystallization of a 30/70 blend.

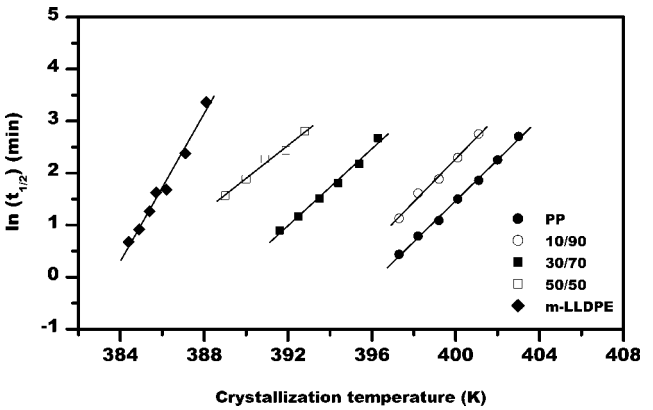

Figure 4 ln $t_{1/2}$ versus T_C for m-LLDPE, PP, and their blends.

m-LLDPE in the PP copolymer. It cannot reflect complete miscibility, however, because m-LLDPE droplets are present within the PP spherulites, and the independence of the PP spherulite growth rate from the m-LLDPE content has been published elsewhere.[31] This suggests that the reduction in T_m^0 can be attributed to the limited solubility of m-LLDPE in PP.

The β values were found to be 1.05 ± 0.1, 1.17 ± 0.1, 1.23 ± 0.1, and 1.32 ± 0.1 for PP and 10/90, 30/70, and 50/50 blends, respectively, indicating that some limited amount of annealing was present in the blends during melting.

Temperature dependence of crystallization

Bulk crystallization rate

The free energy of formation of the critical size nucleus (ΔG_C^*) near T_m, at which nucleation control is rate-determining, can be obtained from the temperature dependence of Z:[46]

$$Z = Z_0 . \exp\left(\frac{-n\Delta G_C^*}{RT_C}\right) \tag{6}$$

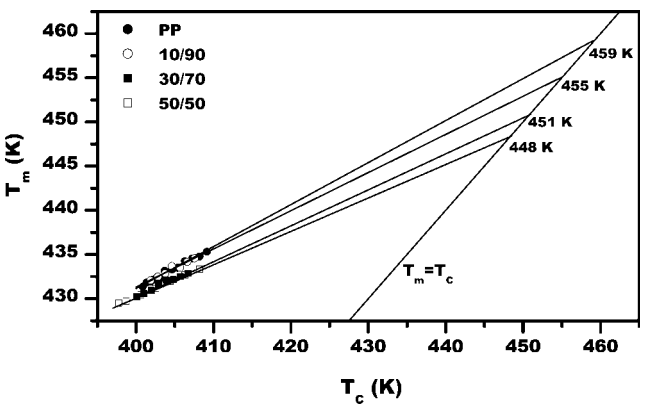

Figure 5 Plots of observed values of T_m versus T_C for PP and the blends.

where Z_0 is a pre-exponential constant related to the composite crystallization rate constant and R is the absolute gas constant. Because primary nucleation has been observed to be sporadic, then

$$\ln Z = \ln Z_0 - \frac{n\Delta G_C^*}{RT_C} \tag{7}$$

A plot of $\frac{1}{n}$ ln Z versus $\frac{1}{T_C}$ is linear, as shown in Figure 6.

The values of ΔG_C^* for m-LLDPE, PP, and 10/90, 30/70 and 50/50 blends were found to be −880 ± 60, −525 ± 30, −550 ± 30, −480 ± 30, and −400 ± 30 kJ/mol, respectively.

Because ΔG_C^* contains a term for the free energy difference between the crystal and molten states at T_C, the calculated values are negative, and the value is greatest for m-LLDPE. The decrease with increasing m-LLDPE content in the blends must reflect a reduction in the free energy of the molten state compared with the free energy of the fold surface by the presence of m-LLDPE in the PP melt. This is considered to be due to some limited miscibility between the two components of the blends.

Spherulite growth rate and rate constant

According to the Turnbull–Fischer theory, the dependence of the crystal growth rate (g) on T_C can be expressed as follows:[45,47]

$$g = \nu_2 \cdot g_0 \exp\left(\frac{-\Delta E_D^*}{RT_C}\right) . \exp\left(\frac{-\Delta G_C^*}{kT_C}\right) \tag{8}$$

where g_0 is a pre-exponential factor generally assumed to be constant or proportional to T_C, ΔE_D^* is the activation energy for the transport of chain segments to the crystal–liquid interface, ν_2 is the volume fraction of the crystallizable polymer, and k is the Boltzmann constant.

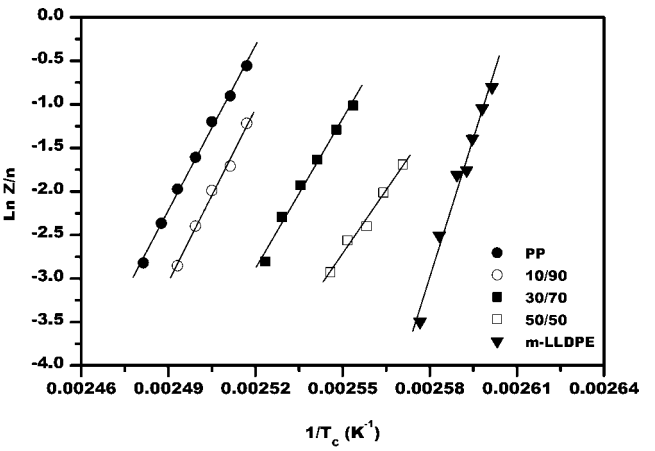

Figure 6 Plot of $\frac{1}{n}$ Ln Z versus $\frac{1}{T_C}$ for m-LLDPE, PP, and their blends.

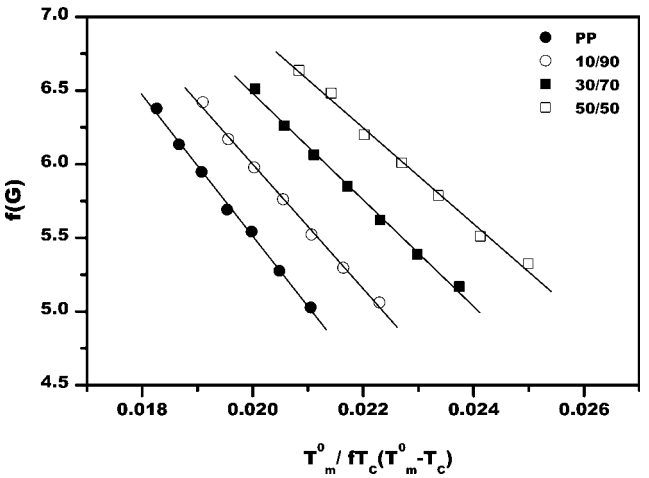

Figure 7 Plot of $f(G)$ versus $T_m^0/(fT_C(T_m^0 - T_C))$ for PP and the blends.

ΔE_D^* was calculated with the Williams–Landel–Ferry equation as follows:[48,49]

$$\Delta E_D^* = \frac{C_1 T_C}{C_2 + T_C - T_g} \tag{9}$$

where T_g is the glass-transition temperature and C_1 and C_2 are constants that generally are considered to be 17,240 J/mol (4120 cal/mol) and 51.6 K, respectively.[50]

ΔG_C^* can be obtained as follows:[51]

$$\Delta G_C^* = \frac{kK_g}{f(T_m^0 - T_C)} \tag{10}$$

$$K_g = \frac{Yb_0\sigma\sigma_e T_m^0}{k\Delta H_u} \tag{11}$$

$$f = \frac{2T_C}{(T_C + T_m^0)} \tag{12}$$

where K_g is the nucleation constant for the growth regime (I–III); ΔH_u is the heat of fusion of the completely crystalline material; and σ and σ_e are the lateral and end surface free energies, respectively. b_0 is the molecular thickness, which was taken to be 0.626 nm for the PP copolymer.[52] The f factor is a correction term that takes into account the temperature dependence of ΔH_u. The difference between T_m^0 and T_C is considered to be the degree of supercooling. The numerical constant Y is equal to 4 when the supercooling is either low (regime I) or high (regime III) and 2 for medium supercooling (regime II).

The spherulitic growth rate (g) is closely related to Z and $t_{1/2}$ as follows:

$$g \propto t_{1/2}^{-1} = \left(\frac{Z}{\ln 2}\right)^{1/n} \tag{13}$$

For the lateral surface energy of linear polymer crystals, the following relation holds:[48,53]

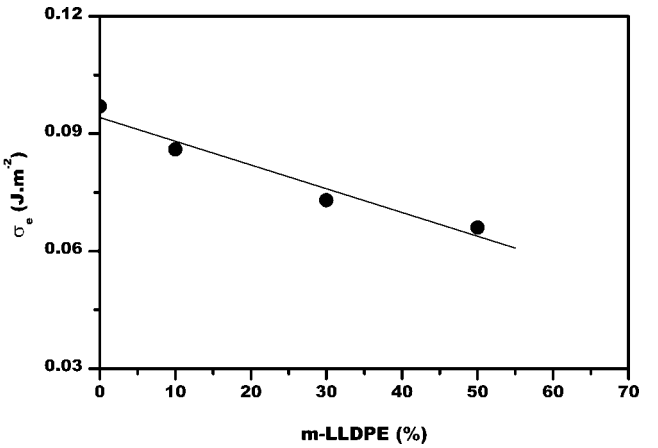

Figure 8 Variation of σ_e of the PP lamellae with the m-LLDPE content.

$$\sigma = 0.1\ b_0.\Delta H_u \tag{14}$$

Combining eqs. (8–14), we can write the following expression applicable to regime III crystallization kinetics:[47,48,54]

$$f(G) = \log g - \log \nu_2 + \frac{17,240}{[2.3R(51.6 + T_C - T_g)]}$$

$$= \log g_0 - \left(\frac{0.4b_0^2\sigma_e}{2.3k}\right)\frac{T_m^0}{fT_C(T_m^0 - T_C)} \tag{15}$$

In this study, regardless of the blend composition, T_g, as measured by dynamic mechanical thermal analysis, was taken to be 268 K. The value for T_g of PP was used because limited solubility was found between the two polymers and also because PP alone crystallized.[50]

The volume fraction was calculated with the densities of the two polymers at 180°C, that is, 759 and 779 kg/m^3 for m-LLDPE and PP, respectively.

Figure 7 shows plots of $f(G)$ against $T_m^0/(fT_C(T_m^0 - T_C))$ for PP and m-LLDPE/PP blends. It is clear that eq. (15) fits the experimental data of the m-

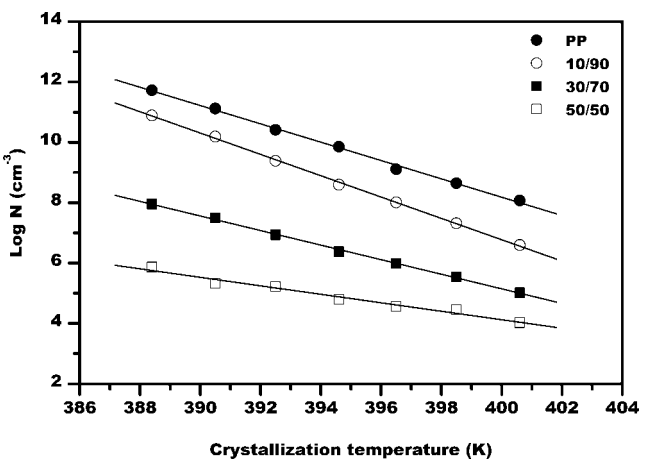

Figure 9 Variation of log N with T_C for PP and the blends.

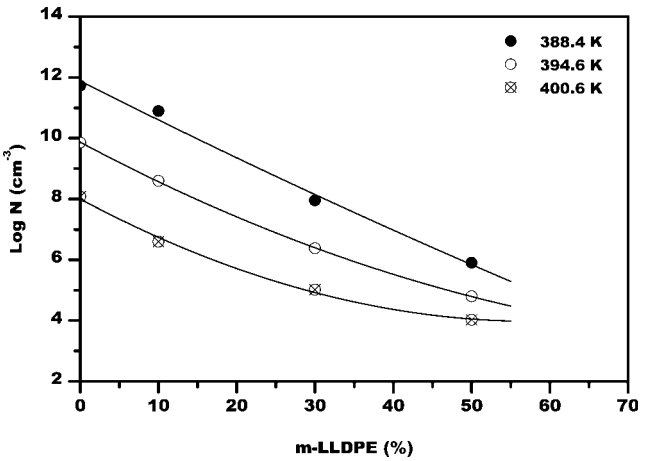

Figure 10 Variation of log N with the m-LLDPE content at three different T_C values.

LLDPE/PP blends well. The values of σ_e and K_g were obtained from the slopes and with eq. (11), respectively. The variation of σ_e with the m-LLDPE content is shown in Figure 8. σ_e decreases with increasing m-LLDPE content, and this again is consistent with some limited solubility of the two components in the molten phase.

Primary nucleation process

For spherulitic growth with instantaneous nucleation, the number of primary nuclei per unit of volume (N) can be calculated according to the following relation:[47,49]

$$Z = \frac{4\pi\rho_c g^3 N}{3\rho_a(1-\lambda(\infty))} \tag{16}$$

where $1 - \lambda(\infty)$ is the crystalline weight fraction at time $t = \infty$ and ρ_c and ρ_a are the densities of 100% crystalline and amorphous polymers, respectively. In eq. (16), Z and N are measured at the same T_C. Figures 9 and 10 reveal that N decreases with increasing T_C at a given composition and also with increasing m-LLDPE content at a constant T_C, respectively. The reduction of the primary nuclei can be attributed to the migration of heterogeneities from PP into m-LLDPE during the mixing process.[48,55] Therefore, for this system in which m-LLDPE does not crystallize, the PP melt contains a smaller number of nucleation particles in the blends than PP alone.

This conclusion is also in agreement with the results obtained by optical microscopy studies, in which it was observed that the number of spherulites for the blends was less than that of PP at a constant temperature.[31] From the results of this study, it can be concluded that the effect of m-LLDPE on reducing the number of primary nuclei can be responsible for reducing the values of the overall kinetic rate constant as m-LLDPE increases in the m-LLDPE/PP blends.

CONCLUSIONS

The isothermal crystallization kinetics and thermal behavior of a PP random copolymer and its three blends with m-LLDPE were studied. T_m^0 and the fold surface free energy of the PP phase in the blends decreased with increasing m-LLDPE in the blend, and this indicated some limited miscibility between the two polymers. The reduction in the overall kinetic rate constant was also attributed to a reduction in the primary nucleation of the PP copolymer upon mixing with m-LLDPE.

References

1. Alizadeh, A.; Munoz-Escalona, A.; Lafuente, P.; Garcia Ramos, J. V.; Martinez-Salazar, J. Polymer 1999, 40, 4345.
2. Munoz-Escalona, A.; Lafuente, P.; Vega, J. F.; Santamaria, A. Polym Eng Sci 1999, 39, 2292.
3. Razavi-Nouri, M.; Hay, J. N. Iran Polym J 2004, 13, 521.
4. Feng, Y.; Jin, X.; Hay, J. N. J Appl Polym Sci 1998, 69, 2469.
5. Li, J.; Shanks, R. A.; Long, Y. J Appl Polym Sci 2000, 76, 1151.
6. Zhou, X.-Q.; Hay, J. N. Polymer 1993, 34, 4710.
7. Hill, M. J.; Oiarzabal, L.; Higgins, J. S. Polymer 1994, 35, 3332.
8. Lovinger, A. J.; Williams, M. L. J Appl Polym Sci 1980, 25, 1703.
9. Nolley, E.; Barlow, J. W.; Paul, D. R. Polym Eng Sci 1980, 20, 364.
10. Tai, C. M.; Li, R. K. Y.; Ng, C. N. Polym Test 2000, 19, 143.
11. Greco, R.; Mucciariello, G.; Ragosta, G.; Martuscelli, E. J Mater Sci 1980, 15, 845.
12. Bartlett, D. W.; Barlow, J. W.; Paul, D. R. J Appl Polym Sci 1982, 27, 2351.
13. Teh, J. W. J Appl Polym Sci 1983, 28, 605.
14. Noel, O. F., III; Carley, J. F. Polym Eng Sci 1984, 24, 488.
15. Rizzo, G.; Spadaro, G. Polym Eng Sci 1984, 24, 264.
16. Yeh, P. L.; Birley, A. W. Plast Rubber Proc Appl 1985, 5, 249.
17. Long, Y.; Stachurski, Z. H.; Shanks, R. A. Polym Int 1991, 26, 143.
18. Flaris, V.; Stachurski, Z. H. J Appl Polym Sci 1992, 45, 1789.
19. Bains, M.; Balke, S. T.; Reck, D.; Horn, J. Polym Eng Sci 1994, 34, 1260.
20. Teh, J. W.; Rudin, A.; Keung, J. C. Adv Polym Technol 1994, 13, 1.
21. Stachurski, Z. H.; Edward, G. H.; Yin, M.; Long, Y. Macromolecules 1996, 29, 2131.
22. Liu, Y.; Truss, R. W. J Appl Polym Sci 1996, 60, 1461.
23. Dong, L.; Olley, R. H.; Bassett, D. C. J Mater Sci 1998, 33, 4043.
24. Li, J.; Shanks, R. A.; Long, Y. Polymer 2001, 42, 1941.
25. Li, J.; Shanks, R. A.; Long, Y. J Appl Polym Sci 2001, 82, 628.
26. Yang, M.; Wang, K.; Ye, L.; Mai, Y.-W.; Wu, J. Plast Rubber Compos 2003, 32, 21.
27. Yang, M.; Wang, K.; Ye, L.; Mai, Y.-W.; Wu, J. Plast Rubber Compos 2003, 32, 27.
28. Rana, D.; Lee, C. H.; Cho, K.; Lee, B. H.; Choe, S. J Appl Polym Sci 1998, 69, 2441.
29. Premphet, K.; Paecharoenchai, W. J Appl Polym Sci 2002, 85, 2412.
30. Razavi-Nouri, M.; Hay, J. N. Polym Eng Sci 2006, 46, 889.
31. Razavi-Nouri, M.; Hay, J. N. Polym Int 2006, 55, 6.
32. Hay, J. N.; Fitzgerald, P. A.; Wiles, M. Polymer 1976, 17, 1015.

33. Bassett, D. C. Principles of Polymer Morphology; Cambridge University Press: Cambridge, England, 1981.
34. Hay, J. N.; Sharma, L. Polymer 2000, 41, 5749.
35. Lu, X.; Hay, J. N. Polymer 2001, 42, 9423.
36. Hay, J. N. In Flow-Induced Crystallization in Polymer Systems; Miller, R. L., Ed.; Gordon & Breach: London, 1979.
37. Hay, J. N.; Mills, P. J. Polymer 1982, 23, 1380.
38. Liu, S.; Yu, Y.; Cui, Y.; Zhang, H.; Mo, Z. J Appl Polym Sci 1998, 70, 2371.
39. Booth, A.; Hay, J. N. Polymer 1969, 10, 95.
40. Hay, J. N.; Sabir, M. Polymer 1969, 10, 203.
41. Martuscelli, E.; Pracella, M.; Crispino, L. Polymer 1983, 24, 693.
42. Jabarin, S. A. J Appl Polym Sci 1987, 34, 97.
43. Yu, J.; He, J. Polymer 2000, 41, 891.
44. Young, R. J.; Lovell, P. A. Introduction to Polymers; Chapman & Hall: London, 1991.
45. Hatakeyama, T.; Liu, Z. Handbook of Thermal Analysis; Wiley: Chichester, England, 1998.
46. Cebe, P.; Hong, S. D. Polymer 1986, 27, 1183.
47. Martuscelli, E.; Pracella, M.; Ye, W. P. Polymer 1984, 25, 1097.
48. Martuscelli, E.; Pracella, M.; Volpe, G. D.; Greco, P. Makromol Chem 1984, 185, 1041.
49. Martuscelli, E. Polym Eng Sci 1984, 24, 563.
50. Martuscelli, E.; Pracella, M.; Avella, M.; Greco, R.; Ragosta, G. Makromol Chem 1980, 181, 957.
51. Urbanovici, E.; Schneider, H. A.; Cantow, H. J. J Polym Sci Part B: Polym Phys 1997, 35, 359.
52. Clark, E. J.; Hoffman, J. D. Macromolecules 1984, 17, 878.
53. Martuscelli, E.; Silvestre, C. Makromol Chem 1989, 190, 2615.
54. Martuscelli, E.; Silvestre, C.; Abate, G. Polymer 1982, 23, 229.
55. Galeski, A.; Bartczak, Z.; Pracella, M. Polymer 1984, 25, 323.